JPP Journal of Pharmacy and Pharmacology

JPP 2004, 56: 529–536

Received September 24, 2003
Accepted January 16, 2004
DOI 10.1211/0022357023196
ISSN 0022-3573

Design, synthesis and properties of novel iron(III)-specific fluorescent probes

Wei Luo, Yong M. Ma, Peter J. Quinn, Robert C. Hider and Zu D. Liu

Abstract

Bidentate chelators such as hydroxypyridinones and hydroxypyranones are highly iron selective. The synthesis of two novel fluorescent probes *N*-[2-(3-hydroxy-2-methyl-4-oxopyridin-1(4*H*)-yl)ethyl]-2-(7-methoxy-2-oxo-2*H*-chromen-4-yl)acetamide (CP600) and *N*-[(3-hydroxy-6-methyl-4-oxo-4*H*-pyran-2-yl)methyl]-2-(7-methoxy-2-oxo-2*H*-chromen-4-yl)acetamide (CP610) is reported. The method involves coupling the bidentate ligands, 3-hydroxypyridin-4-one and 3-hydroxypyran-4-one, with the well-characterised fluorescent probe methoxycoumarin. Fluorescence emission of both probes at 380 nm is readily quenched by Fe^{3+}. The fluorescence was quenched to a greater extent by Fe^{3+} than by Mn^{2+}, Co^{2+}, Zn^{2+}, Ca^{2+}, Mg^{2+}, Na^{+} and K^{+} and to approximately the same extent as Cu^{2+}. Comparison of the fluorescence-quenching ability by a range of metal ions on CP600 and CP610 and the hexadentate chelator, calcein, under in-vitro conditions, demonstrated advantages of the two novel fluorescent probes with respect to both iron(III) sensitivity and selectivity. Chelation of iron(III) by CP600 and CP610 leads to the formation of a complex with a metal-to-ligand ratio of 1:3. Fluorescence is quenched on formation of such complexes. These probes possess a molecular weight less than 400 and thus they are predicted to permeate biological membranes by passive diffusion, and have potential for reporting intracellular organelle labile iron levels.

Introduction

Iron exists in living cells as various chemical species. Cytosolic iron, the form of iron directly affected by complexing agents, is known as the chelatable iron pool or labile iron pool (LIP) (Crichton & Ward 1992; Klausner et al 1993). Its existence was first suggested by Jacobs (1977), who considered it as an intermediate or transitory pool between extracellular iron and cellular iron associated with proteins. Operationally it may comprise of both iron(II) and iron(III) and is loosely associated with a diverse range of ligands, such as organic anions (phosphates and carboxylates), polypeptides and surface components of membranes (e.g. phospholipid head groups). Thus, in the broadest terms, this cellular labile iron pool is comprised of a mixture of chemical forms of iron that can participate in redox-cycling and be scavenged by permeant chelators.

Until recently, attempts to assess levels of LIP have relied on methods involving extraction of cells or tissues with chelators (Sakaida et al 1990) or spectroscopic measurement of chelated iron (Pierre et al 1992; Cooper et al 1996). These methods have either necessitated cell disruption or relatively large amounts of tissue material. In 1995, Cabantchik and co-workers introduced a fluorescent method for assessing the LIP of cells, based on the quenching of calcein (**1**; Figure 1) fluorescence by metal ions (Breuer et al 1995b). Preliminary experiments indicate that this method will provide much useful information relating to cytoplasmic iron(II) levels (Breuer et al 1995a, b; Cabantchik et al 1996). However, calcein is a large hexadentate ligand that only gains entry to the cytoplasmic compartment via its acetoxymethyl ester (calcein-AE). Once hydrolysed, the probe becomes trapped in the cytoplasm and cannot traverse intracellular compartments to gain access to subcellular organelles such as the lysosome where a substantial amount of the cellular LIP is believed to be located (Radisky & Kaplan 1998). A further complication with calcein is its lack of selectivity for iron and the presence of two different coordination sites in the molecule (Thomas et al 1999). To quantitatively

Department of Pharmacy, King's College London, Franklin-Wilkins Building, 150 Stamford Street, London SE1 9NN, UK

Wei Luo, Yong M. Ma, Peter J. Quinn, Robert C. Hider, Zu D. Liu

Correspondence: Z. D. Liu, Department of Pharmacy, King's College London, Franklin-Wilkins Building, 150 Stamford Street, London SE1 9NN, UK.
E-mail: zu.liu@kcl.ac.uk

Acknowledgement and funding: This research project was supported by MRC grant. Dr Hicham H. Khodr at the Department of Pharmacy, King's College London, UK is thanked for providing titration data.

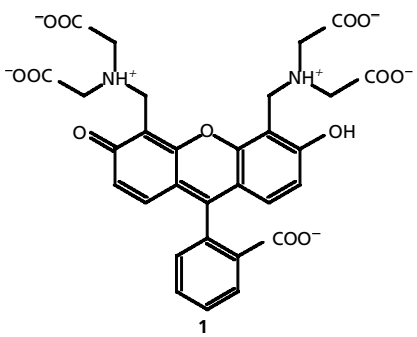

Figure 1 Structure of calcein (**1**).

monitor the distribution of LIP in cells, the specific design of a novel iron-specific fluorescent probe is essential. In this work, two such fluorescent probes are described.

Materials and Methods

Chemistry

Methyl maltol (**2**, Figure 2) was purchased from Cultor Food Science (USA). Kojic acid (**8**, Figure 3) was purchased from Fluka. All other chemicals were obtained from Sigma-Aldrich. Melting points were determined using an Electrothermal IA 9100 Digital Melting Point Apparatus and are uncorrected. ^{1}H NMR spectra were recorded using a Bruker (360 MHz) NMR spectrometer. Chemical shifts (δ) are reported in ppm downfield from the internal standard tetramethylsilane (TMS). Mass spectra (FAB) analyses were carried out by the Mass Spectrometry Facility, School of Health and Life Science (150 Stamford Street, London SE1 9NN, UK). Elemental analyses were performed by Micro analytical laboratories (Department of Chemistry, The University of Manchester, M13 9PL, UK).

*2-Methyl-3-benzyloxypyran-4(1*H*)-one (**3**)*

To a solution of methyl maltol (**2**; 63 g, 0.5 mol) in methanol (500 mL), was added sodium hydroxide (22 g, 0.55 mol) dissolved in water (50 mL), and the mixture was heated to reflux. Benzyl chloride (70 g, 0.55 mol) was added drop-wise over 30 min, and the resulting mixture was refluxed overnight. After removal of solvent by rotary evaporation, the residue was mixed with water (200 mL) and extracted with dichloromethane (3 × 150 mL). The combined extracts were washed with 5% aqueous sodium hydroxide (2 × 200 mL) followed by water (200 mL). The organic fraction was then dried over anhydrous sodium sulfate, filtered and rotary evaporated to yield an orange oil that solidified on cooling. Recrystallization from diethyl ether gave the pure product **3** as colourless needles (87.5 g, 81%): mp 51–52 °C; ^{1}H NMR ($CDCl_3$) δ: 2.12 (s, 3H), 5.11 (s, 2H), 6.25 (d, J = 6 Hz, 1H), 7.28 (s, 5H), 7.47 (d, J = 6 Hz, 1H).

*1-(2-Aminoethyl)-3-(benzyloxy)-2-methylpyridin-4(1*H*)-one (**4**)*

To a solution of **3** (2.16 g, 10 mmol) in water (100 mL), was added ethylenediamine (1.2 g, 20 mmol). The mixture was heated at 70 °C overnight, then extracted with dichloromethane (4 × 100 mL). The combined organic layers were dried over anhydrous sodium sulfate, filtered and rotary evaporated to give brown oil (2.27 g, 88%). ^{1}H NMR ($CDCl_3$) δ: 2.20 (s, 3H), 2.95 (t, J = 6 Hz, 2H), 3.85 (t, J = 6 Hz, 2H), 5.16 (s, 2H), 6.32 (d, J = 7.8 Hz, 1H), 7.31 (d, J = 7.8 Hz, 1H), 7.34 (s, 5H).

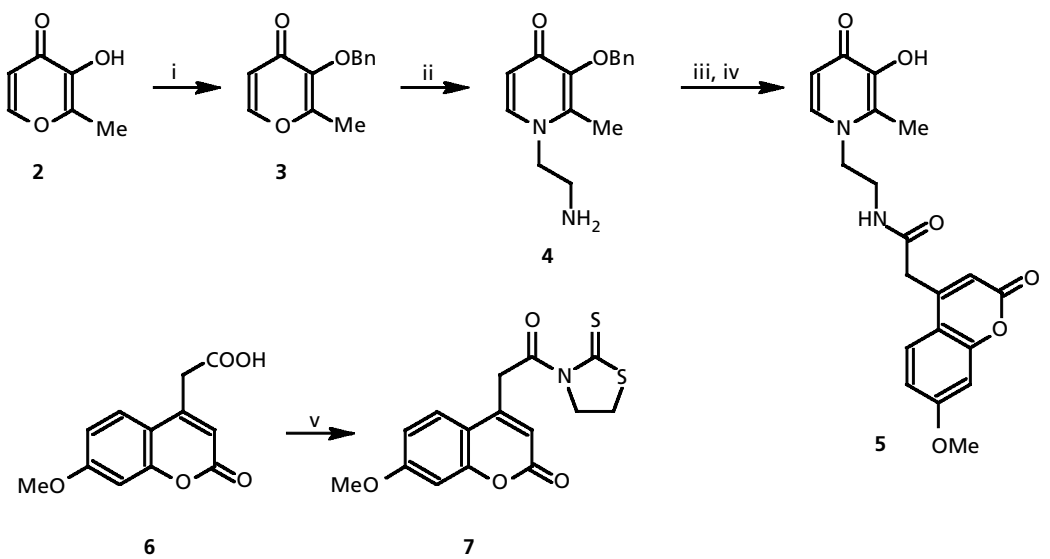

Figure 2 Compounds **2**–**7**. Reagents and conditions: i, BnBr, NaOH, MeOH/H_2O, 70 °C, 81%; ii, 1,2-diaminoethane, NaOH, EtOH/H_2O, 70–80 °C, 88%; iii, 7, CH_2Cl_2, 25 °C, 82%; iv, H_2, 5%Pd-C (cat), EtOH, 25 °C, 82%; v, DCC, DMAP and 2-mercaptothiazoline, 25 °C, 60%.

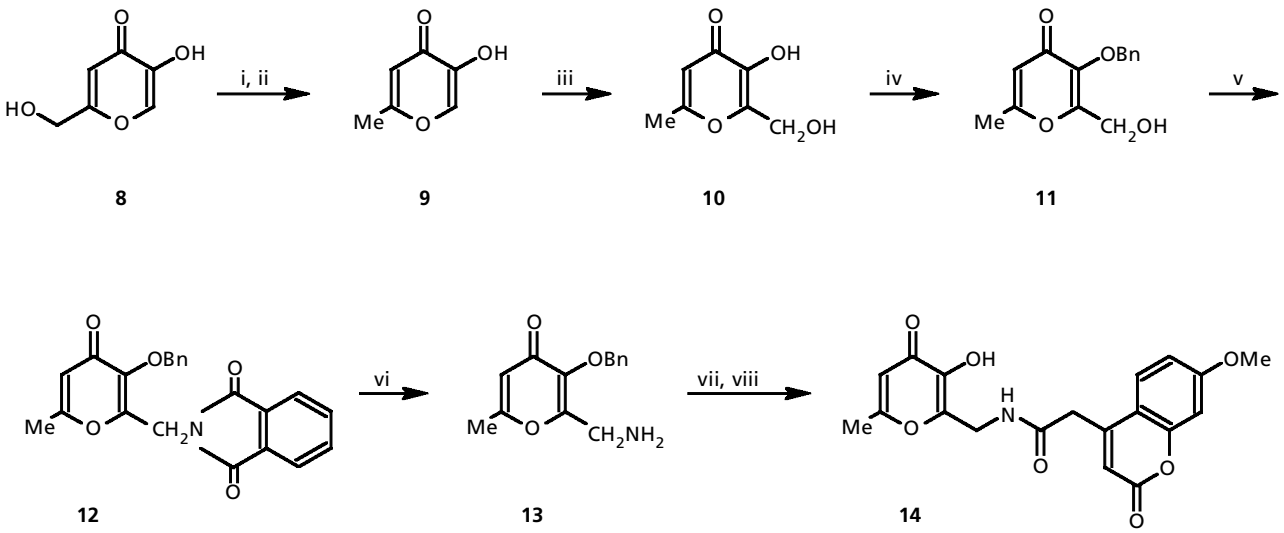

Figure 3 Compounds **8**–**14**. Reagents and conditions: i, $SOCl_2$, 25 °C, 80%; ii, Zn/HCl, H_2O, 65–70 °C, 74%; iii, HCHO, NaOH, H_2O, 25 °C, 92%; iv, BnBr, NaOH, MeOH/H_2O, 70 °C, 80%; v, PPh_3, Phthalimide, DEAD, THF, 25 °C, 73%; vi, 5.5% aqueous hydrazine, EtOH, 70 °C, 65%; vii, 7, CH_2Cl_2, 25 °C, 61%; viii, H_2, 5%Pd-C (cat), EtOH, 25 °C, 63%.

*N-[2-(3-Hydroxy-2-methyl-4-oxopyridin-1(4*H*)-yl) ethyl]-2-(7-methoxy-2-oxo-2*H*-chromen-4-yl) acetamide hydrochloride (**5**)*

To a vigorously stirred suspension of **6** (2.34 g, 10 mmol) in dichloromethane (100 mL), was added dicyclohexylcarbodiimide (DCCI) (2.3 g, 11 mmol), 2-mercaptothiazoline (1.32 g, 11 mmol) and a catalytic amount of 4-dimethylaminopyridine (DMAP) (50 mg). The mixture was stirred for 24 h, the white precipitate *N*,*N*′-dicyclohexylurea (DCU) was filtered from the yellow solution and to the filtrate was added the amine **4** (2.58 g, 10 mmol) and the reaction mixture allowed to stir overnight. The dichloromethane layer was washed with 0.1 M sodium hydroxide solution (3 × 50 mL) and water (50 mL), dried over anhydrous sodium sulfate, and the solvent removed in-vacuo. The crude product was further purified by column chromatography on silica gel (eluant: methanol–chloroform, 1:9 v/v) to afford a white solid *N*-[2-(3-benzoxy-2-methyl-4-oxopyridin-1 (*4H*)-yl)ethyl]-2-(7-methoxy-2-oxo-*2H*-chromen-4-yl)acetamide (2.32 g, 49%): mp 202–203 °C; ^{1}H NMR ($CDCl_3$) δ: 2.05 (s, 3H), 3.54 (s, 2H), 3.72–3.84 (m, 7H), 4.81 (s, 2H), 5.90 (d, J = 7.8 Hz, 1H), 6.06 (s, 1H), 6.70–6.85 (m, 2H), 7.18 (s, 5H), 7.38 (d, J = 9.0 Hz, 1H), 8.10 (d, J = 7.8 Hz, 1H). m/z: 475 $(M+1)^+$. A solution of this white solid in *N*,*N*-dimethylformamide (DMF) was subjected to hydrogenolysis in the presence of Pd/C 5% (w/w) catalyst for 5 h. The catalyst was removed by filtration and the filtrate was acidified to pH 1 with concentrated HCl. After removal of the solvents in-vacuo, the residue was purified by recrystallization from methanol to afford a white solid **5** (89%): mp 256–258 °C. ^{1}H NMR (360 MHz, DMSO-d_6) δ: 2.51 (s, 3H), 3.69 (s, 2H), 4.39 (t, 2H, J = 5.7 Hz), 6.96 (dd, 1H, J = 8.7 8.6 Hz), 7.2 (d, 1H, J = 6.9 Hz), 8.07 (d, 1H, J = 7.0 Hz), 3.50 (q, 2H, J = 5.7 Hz), 3.87 (s, 3H), 6.23 (s, 1H), 6.98 (d, 1H, J = 2.3 Hz), 7.56 (d, 1H, J = 8.6 Hz), 8.61 (t, 1H, J = 5.4 Hz); ^{13}C NMR (90 MHz, DMSO-d_6) δ: 168.7, 162.7, 160.4, 159.2, 155.3, 150.8, 143.2, 141.8, 139.0, 126.9, 113.3, 112.8, 112.4, 110.7, 101.3, 56.4, 55.4, 38.8, 12.9; MS (ES): m/z, 385 $[M-Cl]^+$; Anal. Calcd. for $C_{20}H_{21}ClN_2O_6$: C, 57.08; H, 5.03; Cl, 8.42; N, 6.66%. Found: C, 56.92; H, 4.98; Cl, 8.40; N, 6.64%.

*2-Methyl-5-hydroxypyran-4(1*H*)-one (**9**)*

Kojic acid (**8**; 14.2 g, 100 mmol) was dissolved in distilled thionyl chloride (60 mL) and stirred for 1 h, after which time a pale yellow crystalline mass formed. The product was collected by filtration and washed with petroleum ether to afford a pale yellow amorphous powder (11 g, 80%): mp 164–164.5 °C (lit. value 166–168 °C); ^{1}H NMR (DMSO-d_6) δ: 4.65 (s, 2H), 6.62 (s, 1H), 8.23 (s, 1H), 8.80 (br s, 1H). The above powder (30 g, 0.187 mol) was added to 100 mL of distilled water and heated to 50 °C with stirring. Zinc dust (24.4 g, 0.375 mol) was added followed by the drop-wise addition of concentrated HCl (56.1 mL) over 1 h with vigorous stirring, maintaining the temperature at 70–80 °C. The reaction mixture was stirred for a further 3 h at 70 °C. The excess zinc was removed by filtration (at 70 °C) and the filtrate was extracted with dichloromethane (5 × 200 mL). The combined organic extracts were dried over anhydrous sodium sulfate, filtered and concentrated in-vacuo to yield the crude product. Recrystallisation from isopropanol afforded colourless plates **9** (17.4 g, 74%). mp 149–150 °C; ^{1}H NMR (DMSO-d_6) δ: 2.25 (s, 3H), 6.14 (s, 1H), 6.70 (br s, 1H), 7.63 (s, 1H).

*2-Hydroxymethyl-3-hydroxy-6-methyl-pyran-4(1*H*)-one (**10**)*

Allomaltol (**9**; 12.6 g, 100 mmol) was added to an aqueous solution of sodium hydroxide (4.4 g, 110 mmol) in distilled water (100 mL) and stirred at room temperature for 5 min. Formaldehyde solution (35%, 9 mL) was added drop-wise

over 10 min and the solution was stirred for 12 h. Acidification to pH 1 using concentrated HCl and cooling to 3–5 °C for 12 h gave a crystalline deposit (14.4 g, 92%); mp 157 °C; ^{1}H NMR (DMSO-d_6) δ: 2.23 (s, 3H), 4.38 (s, 2H), 4.90 (br s, 1H), 6.20 (s, 1H), 8.80 (br s, 1H).

*2-Methyl-3-benzyloxypyran-4(1H)-one (**11**)*
To a solution of **10** (15.6 g, 0.1 mol) in methanol (100 mL), was added sodium hydroxide (4.4 g, 0.11 mol) dissolved in water (10 mL), and the mixture was heated to reflux. Benzyl chloride (14 g, 0.11 mol) was added drop-wise over 30 min, and the resulting mixture was refluxed overnight. After removal of solvent by rotary evaporation, the residue was mixed with water (200 mL) and extracted with dichloromethane (3 × 150 mL). The combined extracts were washed with 5% aqueous sodium hydroxide (2 × 200 mL) followed by water (200 mL). The organic fraction was then dried over anhydrous sodium sulfate, filtered and rotary evaporated to yield the crude product as a yellow crystalline solid. Recrystallization from dichloromethane–petroleum ether (40/60) afforded a white crystalline solid (19.7 g, 80%): m.p. 113–114 °C;. ^{1}H NMR ($CDCl_3$) δ: 2.20 (s, 3H), 2.63 (br s, 1H), 4.28 (s, 2H), 5.15 (s, 2H), 6.15 (s, 1H), 7.36 (s, 5H).

*6-Methyl-2-phthalimidomethyl-3-benzyloxypyran-4-one (**12**)*
To a solution of triphenyl phosphine (6.3 g, 24 mmol) and phthalimide (3.5 g, 24 mmol) in THF (100 mL), was added **11** (4.92 g, 20 mmol), and the mixture was cooled to 0 °C in an ice bath. Diethyl azodicarboxylate (4.2 g, 24 mmol) was added drop-wise with stirring over 30 min, after which the reaction mixture was allowed to warm slowly to room temperature and to stand overnight. After removal of solvent by rotary evaporation, the product was purified by column chromatography on silica gel to furnish a white powder (73%): mp 223–225 °C; ^{1}H NMR ($CDCl_3$) δ: 2.10 (s, 3H), 4.64 (s, 2H), 5.16 (s, 2H), 6.03 (s, 1H), 7.10–7.70 (m, 9H).

*2-Aminomethyl-6-methyl-3-benzyloxy-pyran-4-one (**13**)*
To a solution of **12** (5.6 g, 15 mmol) in ethanol (96% 50 mL), was added hydrazine monohydrate (0.8 g, 16 mmol). After being refluxed for 3 h, the reaction mixture was chilled to 0 °C, acidified to pH 1, concentrated in-vacuo and the residue was re-dissolved in distilled water (50 mL), adjusted to pH 12 with 10 M sodium hydroxide and extracted with dichloromethane (3 × 100 mL). The combined organic extracts were dried over anhydrous sodium sulfate, and the solvent was removed under reduced pressure to yield a brown oil. Purification by column chromatography on silica gel furnished an orange oil (2.39 g, 65%); ^{1}H NMR ($CDCl_3$) δ: 2.17 (s, 3H), 3.41 (s, 2H), 5.05 (s, 2H), 6.02 (s, 1H), 7.20 (s, 5H).

*N-[(3-Hydroxy-6-methyl-4-oxo-4H-pyran-2-yl) methyl]-2-(7-methoxy-2-oxo-2H-chromen-4-yl) acetamide (**14**)*
The method for the synthesis of **14** was the same as that for **5** (see above) (38%); mp 262–263 °C. ^{1}H NMR (360 MHz, DMSO-d_6) δ: 2.17 (s, 3H), 3.85 (s, 3H), 6.21 (s, 1H), 6.94 (dd, 1H, J = 8.8–8.9Hz), 7.67 (d, 1H, J = 8.9Hz), 9.07 (brs, 1H), 3.73 (s, 2H), 4.29 (d, 2H, J = 5.5Hz), 6.25 (s, 1H), 7.00 (d, 1H, J = 2.4Hz), 8.73 (t, 1H, J = 5.4Hz); ^{13}C NMR (90 MHz, DMSO-d_6) δ: 173.9, 168.3, 164.8, 162.7, 160.5, 155.3, 151.3, 146.9, 142.1, 126.8, 112.9, 112.8, 112.5, 111.7, 101.2, 56.3, 39.0, 35.9, 19.5; MS (ES): m/z, 372 $[M + 1]^+$; Anal. Calcd. for $C_{19}H_{17}NO_7$: C, 61.45; H, 4.61; N, 3.77%. Found: C, 61.35; H, 4.65; N, 3.73%.

Physicochemical properties

Optical characterisation
The UV/VIS spectra of the two probes were recorded using a Perkin-Elmer spectrophotometer (type UV/VIS Lambda 2S) and a Perkin-Elmer spectrofluorometer (type LS 50B) was used to record fluorescence emission spectra operating at a scan rate of 120 nm min^{-1}. Spectra were not corrected for light intensity or detector sensitivity. Data were recorded on-line and analysed by Excel software on a PC computer. Fluorescence quenching measurements were performed in aqueous solution (pH 7.0) at 22 °C. Comparison of the effects on fluorescence emission effects of Fe^{3+} ($FeCl_3$) and of Na^+ (NaCl), K^+ (KCl), Mg^{2+} ($MgCl_2$), Ca^{2+} ($CaCl_2$), Mn^{2+} ($MnCl_2$), Cu^{2+} ($CuCl_2$), Co^{2+} ($CoCl_2$), and Zn^{2+} ($ZnCl_2$) were made using the two novel probes.

Recording of fluorescence quantum yield
The fluorescence quantum yield (Φ_F) is the ratio of photons absorbed to photons emitted by fluorescence. The quantum yield gives the probability of the excited state being deactivated by fluorescence rather than by another, non-radiative, mechanism. The most reliable method for recording Φ_F is the comparative method of Williams et al (1983), which involves the use of well-characterised standard samples with known Φ_F values. Adopting this method, the general experimental considerations follow:

Standard samples. The standard samples should be chosen to ensure that they absorb at the excitation wavelength of choice for the test sample, and, if possible, emit in a similar region to the test sample. The standard samples must be well characterised and suitable for such use. For these reasons, quinine and harmane were adopted as standards.

Cuvettes. Standard 10-mm path length fluorescence cuvettes were used for fluorescence measurements.

Concentration range. To minimise re-absorption effects (Dhami et al 1995), absorbances in the 10-mm fluorescence cuvette should never exceed 0.1 at and above the excitation wavelength. Above this level, non-linear effects may be observed due to inner filter effects, and the resulting quantum yield values may be perturbed.

Sample preparation. It is vital that all glassware is kept scrupulously clean, and solvents must be of spectroscopic grade and checked for background fluorescence.

Sample fluorescence. The fluorescence for each sample was recorded for a range of 5 concentrations (absorbance

values in the range 0.02–0.1). Plots of integrated fluorescence intensity (I_F) vs absorbance (A) were recorded.

Calculation of fluorescence quantum yield

The gradient of each graph (I_F vs A) is proportional to the quantum yield of the sample under investigation. Absolute values were calculated using standard samples, which have a known fluorescence quantum yield, given by equation 1.

$$\Phi_X = \Phi_{ST}(\mathrm{Grad}_X/\mathrm{Grad}_{ST})(\eta^2_X/\eta^2_{ST}) \quad (1)$$

Where the subscripts ST and X denote standard and test, respectively, Φ is the fluorescence quantum yield, Grad is the gradient from the plot of integrated fluorescence intensity vs absorbance and η is the refractive index of the solvent.

The two standard compounds were cross-calibrated using this equation. This was achieved by calculating the quantum yield of each standard sample relative to the other. Once the standard samples are cross-calibrated, the quantum yield values for the test samples can then be calculated, using the same equation. For each test sample, two Φ_F values will be obtained by virtue of the use of two standards. The average of these two values represents the quantum yield of the test sample and is the value reported in this study.

Determination of distribution coefficients

Distribution coefficients ($D_{7.4}$) of the chelators between 1-octanol and MOPS buffer (pH 7.4) were determined at $25 \pm 0.5\,^{\circ}C$, using an automated continuous flow technique that provided accurate and reproducible measurements (Dobbin et al 1993; Rai et al 1998; Liu et al 1999). The compound to be examined was dissolved in a known volume (normally 25–50 mL) of MOPS buffer (saturated with octanol) so as to give an absorbance of 0.5–1.5 absorbance units at a preselected wavelength (~280 nm). After equilibrium was reached, a small amount of octanol (saturated with MOPS buffer pH 7.4) was added and re-equilibration assessed. This cycle was repeated until a predefined total volume of added octanol was reached. The aqueous phase was separated from the two-phase system (1-octanol/MOPS buffer, pH 7.4) by means of a hydrophilic cellulose filter (5 μm diameter, 589/3 Blauband filter paper; Schleicher & Schuell). The flow rate of the aqueous circuit was limited to 1 mL min^{-1}. The distribution coefficient was calculated for each octanol addition.

Determination of affinity constants

Equilibrium constants of protonated ligands were determined using an automated system, consisting of a Metrohm 765 dosimat, a Perkin-Elmer Lambda 5 Spectrophotometer, a METTLER TOLEDO MP 230 pH meter, combined Sirius electrode and a Dell PC computer as controller of the integrated system. This system is capable of performing simultaneous potentiometric and spectrophotometric measurements (Dobbin et al 1993; Rai et al 1998; Liu et al 1999). Titrations were carried out in a jacketed vessel maintained at $25 \pm 0.5\,^{\circ}C$ under an argon atmosphere fitted with a recirculatory solution path through a 1-mm flow-through cell in the spectrophotometer light path. Solutions were titrated with 0.3 mL of 0.2 M KOH using 0.01-mL increments dispensed from the dosimat. A blank titration of 0.1 M KCl (25 mL) acidified with 0.15 mL of 0.2 M HCl was carried out to determine the electrode response slope and zero using Gran's plot method. The titration was repeated in the presence of ligand. The data obtained from titration were subjected to non-linear least-square regression analysis (Taylor et al 1988).

Iron(III) stability constants of the ligands were determined from the spectrophotometric titration of the metal–ligand system using the pK_a values, electrode slope and electrode zero determined above (Liu et al 1999). The analytical equipment used was similar to that used for pK_a determination but, to maintain sufficient sensitivity, a 1-cm path length UV flow-cell was utilised. After electrode calibration, the solution was re-acidified to pH 1.5–2.0 by adding concentrated HCl. Iron(III) stock solution (atomic absorption standard, Aldrich) and the test ligand were then added to give a final ligand-to-iron(III) ratio of about 10:1. A pre-adjusted, programmed, autoburette was used for the addition of 0.2 M KOH solution. The resulting spectrophotometric titration curve was then subjected to non-linear least-squares regression analysis for the determination of stability constants.

Results and Discussion

The optical properties of CP600 and CP610 are similar. There are two absorbance peaks observed in UV/VIS spectra of CP600 and CP610 (Figure 4). The CP600 absorbance peak of 285 nm is associated with the hydroxypyr-

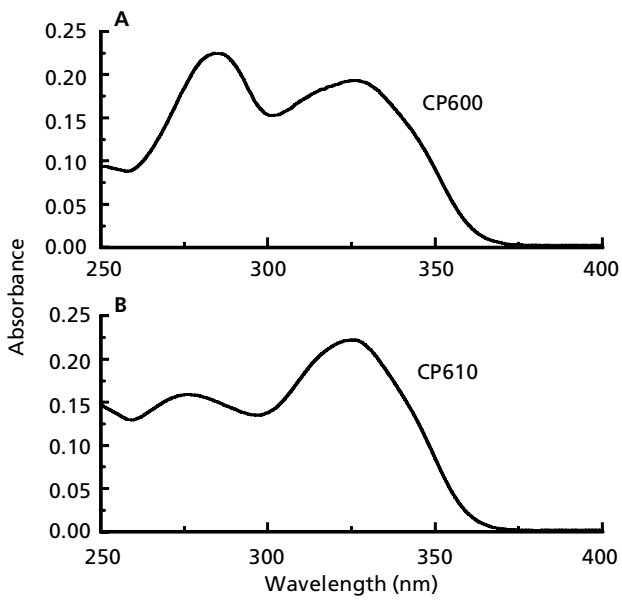

Figure 4 Absorbance spectra of CP600 (A; 15 μM) and CP610 (B; 15 μM) in aqueous solution, pH 7.0. No. of replicates, n = 3.

idinone and the 277-nm peak of CP610 is associated with the hydroxypyranone. Both CP600 and CP610 possess an absorbance peak at 325 nm, which is due to methoxycoumarin and emits fluorescence. CP600 and CP610 have the same excitation wavelength of 325 nm and same emission wavelength of 380 nm. The quantum yield of CP610 is about four fold that of CP600.

The physicochemical properties of the probes are summarised in Table 1. Both CP600 and CP610 are relatively small in size, their molecular weights being 421 and 371, and their LogP values are 0 and 0.2, respectively. These physical features are favourable for efficient intracellular distribution according to Lipinski's Rule-of-Five guidelines (Bajorath 2002). The Logβ_3 values of CP600 and CP610 are both sufficiently large to ensure that iron(III) is efficiently bound to these ligands at pH 7.4. However, the β_3 value of CP600 is 10^4-fold greater than that of CP610.

Metal sensitivity of CP600- and CP610-fluorescence

The fluorescent emission intensity of CP600 was found to be sensitive to the presence of metal ions and a clear fluorescence quenching was observed on adding ferric chloride solution. The effect of increasing iron(III) concentration on the fluorescence emission spectrum of CP600 is shown in Figure 5A. It was found that when the metal-to-ligand ratio was less than 1:3, there was a linear relationship between the fluorescence intensity and the concentration of iron(III) (Figure 5B). At ratios of metal-to-ligand greater than 1:3 no additional quenching of fluorescence was observed. This is consistent with fluorescence quenching of the bidentate ligand CP600 by

Table 1 Physicochemical properties and molecular descriptors of CP600 and CP610.

	CP600	CP610
Molecular weight (Da)	421	371
Excitation wavelength (nm)	325	325
Emission wavelength (nm)	380	380
ε (10^3 M^{-1} cm^{-1})	12.2 ± 0.1	12.7 ± 0.1
Φ_F	0.036 ± 0.002	0.182 ± 0.005
$D_{7.4}$	1.19 ± 0.05	1.45 ± 0.05
LogP	0.08 ± 0.02	0.22 ± 0.02
pK_a	4.28 ± 0.05 10.25 ± 0.05	8.26 ± 0.05
Logβ_3	37.9 ± 0.5	33.1 ± 0.5
pFe	20.5 ± 0.2	19.5 ± 0.2

ε, Molar extinction coefficient of the ligand; Φ_F, quantum yield; $D_{7.4}$, the measured distribution coefficients of the ligand between 1-octanol and MOPS buffer (pH 7.4); LogP, the logarithm of the partition coefficients of the ligand between 1-octanol and MOPS buffer (pH 7.4); pK_a, the negative logarithm of the equilibrium constant of the protonated ligand; Logβ_3, the logarithm of the cumulative iron(III) stability constant for the ligand; pFe, the negative logarithm of the concentration of the free iron(III) in solution, calculated for total [ligand] = 10^{-5} M, total [iron] = 10^{-6} M at pH 7.4. Data are means ± s.d., n = 3.

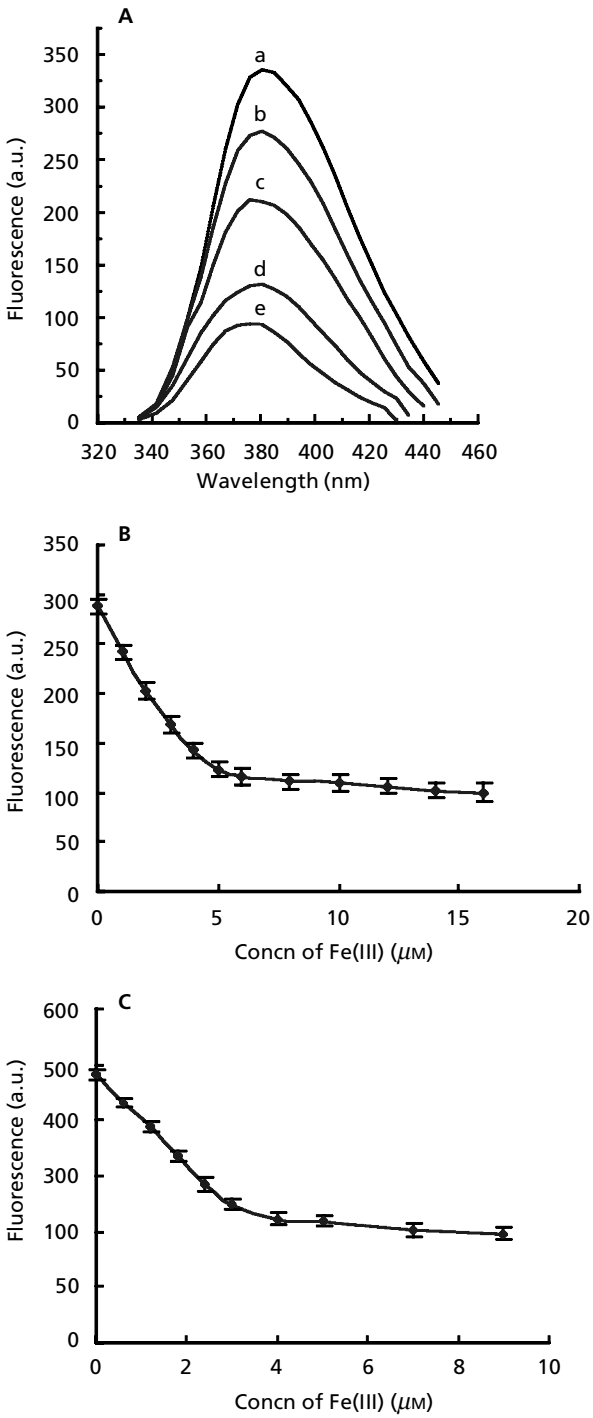

Figure 5 A. Metal sensitivity of fluorescence emission spectra of CP600 (15 μM) in aqueous solution, pH 7.0; λ_{ex} = 325 nm. Curve a, fluorescence emission spectra; b–e, fluorescence quenching resulting from the presence of iron(III); b, 2 μM iron(III); c, 4 μM iron(III); d, 6 μM iron(III); e, 15 μM iron(III). No. of replicates, n = 3. B. Fluorescence (λ_{em} = 380 nm) of CP600 (15 μM) quenched by varying concentration of iron(III) in aqueous solution, pH 7.0. C. Fluorescence (λ_{em} = 380 nm) of CP610 (6 μM) quenched by varying concentration of iron(III) in aqueous solution, pH 7.0. Data are means ± s.d., n = 5.

formation of a 1:3 iron(III) complex. The results of fluorescence quenching of CP610 in the presence of iron(III) are shown in Figure 5C. It was clear that the fluorescence of this compound was quenched in a manner different to that observed with CP600, the maximum quenching of fluorescence occurring at a stoichiometry of 1:2 iron to ligand.

Typical steady-state values of cellular LIP in cells are in the lower micromolar range (Epsztejn et al 1997). These values increase following iron loading (Zanninelli et al 2002) and suppression of ferritin expression (Kakholn et al 2001). In contrast, they decrease following iron starvation (Breuer et al 1996), subsequent to the addition of chelators (Cabantchik et al 1996) or over-expression of ferritin (Epsztejn et al 1999).

The parameters established in this study show, from the quenching curve of CP600 (Figure 6), that there is a linear relationship with iron(III) in the concentration range of iron(III) 0–1.0 μM when the concentration of ligand CP600 is 3 μM. This suggests that, in principle, the bidentate ligand CP600 is able to quantitatively assess physiological levels of cellular LIP.

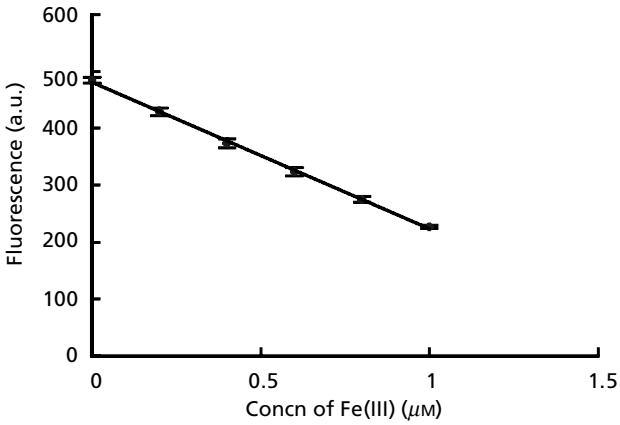

Figure 6 Linear relationship of CP600 (3 μM) fluorescence ($\lambda_{em} = 380$ nm) with iron(III) over the concentration range of iron(III) 0–1.0 μM, pH 7.0. Data are means ± s.d., n = 5.

Metal selectivity of CP600 and CP610

The effects of Fe^{3+} ($FeCl_3$), Na^+ (NaCl), K^+ (KCl), Mg^{2+} ($MgCl_2$), Ca^{2+} ($CaCl_2$), Mn^{2+} ($MnCl_2$), Cu^{2+} ($CuCl_2$), Co^{2+} ($CoCl_2$) and Zn^{2+} ($ZnCl_2$) on the fluorescence intensity of CP600 and CP610 are presented in Figure 7. Studies were also undertaken with calcein to compare the selectivity of quenching with the two fluorescent iron(III) chelators. The fluorescence of CP600 (15 μM) and CP610 (7.5 μM) were quenched by 70% and 30%, respectively, in the presence of iron(III) at a metal-to-ligand ratio of 1:3. The fluorescence quenching by other metals at identical ratios was less than 10%, with the exception of copper(II). In contrast, the quenching of calcein (0.5 μM) fluorescence under the same conditions with a metal-to-ligand ratio of 1:1 was found to be quite marked. Significant quenching was observed in the presence of Cu^{2+} (90%), Co^{2+} (60%), Mn^{2+} (40%) and Zn^{2+} (13%), all of which exceeded that induced by Fe^{3+}, where the extent of fluorescence quenching was surprisingly low, only 6%. The fluorescence of the chelators CP600 and CP610 was quenched by Cu^{2+} at a metal-to-ligand ratio of 1:3 to the extent of 48% and 63%, respectively. It should be noted, however, that the intracellular free Cu^{2+} pool is vanishingly small and certainly less than 10^{-12} M (Rae et al. 1999). In practice therefore, the presence of free copper(II) can be neglected in normal cells and is unlikely to influence CP600 and CP610 fluorescence.

It is clear that the iron(III) chelators CP600 and CP610 are more selective sensors of iron(III) than calcein. Both CP600 and CP610 bind iron(III) more tightly than iron(II)

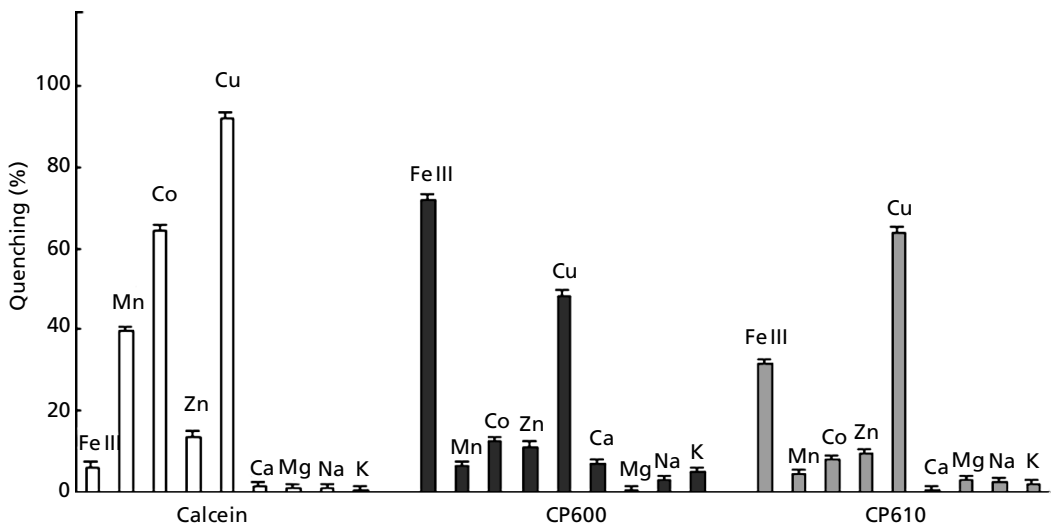

Figure 7 Metal-cation-induced fluorescence quenching of chelator calcein (0.5 μM), metal-to-ligand ratio of 1:1, $\lambda_{ex} = 494$ nm, $\lambda_{em} = 506$ nm; CP600 (15 μM), metal-to-ligand ratio of 1:3, $\lambda_{ex} = 325$ nm, $\lambda_{em} = 380$ nm; CP610 (7.5 μM), metal-to-ligand ratio of 1:3, $\lambda_{ex} = 325$ nm, $\lambda_{em} = 380$ nm, pH 7.0. Data are means ± s.d., n = 5.

and, consequently, will facilitate the autoxidation of iron(II) under aerobic conditions (Hider & Hall 1991). Therefore, these novel probes are predicted to be capable of monitoring the combined levels of iron(II) and iron(III). In contrast, calcein is reported only to monitor iron(II) under biological conditions (Breuer et al 1995a, b).

Conclusion

In summary, two novel iron(III)-selective fluorescent probes, CP600 and CP610, have been synthesised. These probes are highly selective for tribasic cations and will not suffer interference from physiological levels of dibasic cations such as zinc(II), magnesium(II) and calcium(II). Both probes are neutral at pH 7.4 and, by virtue of their relatively small molecular size (MW < 400), are predicted to rapidly penetrate biological membranes by passive diffusion. This analysis has recently been confirmed with both CP600 and CP610 having been demonstrated to rapidly permeate human erythrocyte membranes (unpublished observations). They have the potential for being monitored by their non-charged nature at pH 7.0 and fluorescent properties and therefore to quantify the intracellular distribution of labile iron. These novel fluorescent probes may facilitate the understanding of the nature and the distribution of the labile iron pool in biological systems, particularly in intracellular organelles such as the lysosome.

References

Bajorath, J. (2002) Integration of virtual and high-throughput screening. *Drug Discovery* **1**: 882–894

Breuer, W., Epsztejn S., Cabantchik, Z. I. (1995a) Iron acquired from transferrin by K562 cells is delivered into a cytoplasmic pool of chelatable iron(II). *J. Biol. Chem.* **270**: 24209–24215

Breuer, W., Epsztejn, S., Milgram P., Cabantchik, Z. I. (1995b) Transport of iron and other transition metals into cells as revealed by a fluorescent probe. *Am. J. Physiol. Cell Physiol.* **268**: C1354–C1361

Breuer, W., Epsztejn, S., Cabantchik, Z. I. (1996) Dynamics of the cytosolic chelatable iron pool of K562 cells. *FEBS Lett.* **382**: 304–308

Cabantchik, Z. I., Glickstein, H., Milgram P., Breuer W. (1996) A fluorescence assay for assessing chelation of intracellular iron in a membrane model system and in mammalian cells. *Anal. Biochem.* **233**: 221–227

Cooper, E., Lynagh, G. R., Hoyes, K. P., Hider, R. C., Cammack, R., Porter, J. B. (1996) The relationship of intracellular iron chelation to the inhibition and regeneration of human ribonucleotide reductase. *J. Biol. Chem.* **271**: 20291–20299

Crichton, R. R., Ward, R. J. (1992) Chemistry and molecular biology of iron and iron-binding proteins: structure and molecular biology of iron-binding proteins and the regulation of free iron pools. In: Laufer, R. B. (ed.) *Iron and human diseases.* CRC Press, Boca Raton, FL, pp 23–76

Dhami, S., Mello, A. J., Rumbles, G., Bishop, S. M., Phillips, D., Beeby, A. (1995) Phthalocyanine fluorescence at high concentration: dimers or reabsorption effect? *Photochem. Photobiol.* **61**: 341–346

Dobbin, P. S., Hider, R. C., Hall, A. D., Taylor, P. D., Sarpong, P., Porter, J. B., Xiao, G., van der Helm, D. (1993) Synthesis, physicochemical properties, and biological evaluation of N-substituted 2-alkyl-3-hydroxy-4(1H)-pyridinones: orally active iron chelators with clinical potential. *J. Med. Chem.* **36**: 2448–2458

Epsztejn, S., Kakhlon, O., Glickstein, H., Breuer, W., Cabantchik, Z. I. (1997) Fluorescence analysis of the labile iron pool of mammalian cells. *Anal. Biochem.* **248**: 31–40

Epsztejn, S., Glickstein, H., Picard, V., Slotki, I. N., Breuer, W., Beaumont, C., Cabantchik, Z. I. (1999) H-Ferritin subunit overexpression in erythroid cells reduces the oxidative stress response and induces multidrug resistance properties. *Blood* **94**: 3593–3603

Hider, R. C., Hall, A. D. (1991) 2 Clinically useful chelators of tripositive elements. *Prog. Med. Chem.* **28**: 41–173

Jacobs, A. (1977) An intracellular transit iron pool. In: *CIBA foundation symposium 51*. Elsevier, New York, pp 91–106.

Kakholn, O., Gruenbaum, Y., Cabantchik, Z. I. (2001) Repression of ferritin expression increases the labile iron pool, oxidative stress, and short-term growth of human erythroleukemia cells. *Blood* **97**: 2863–2871

Klausner, R. D., Rouault, T. A., Harford, J. B. (1993) Regulating the fate of mRNA: the control of cellular iron metabolism. *Cell* **72**: 19–28

Liu, Z. D., Khodr, H. H., Liu, D. Y., Lu, S. L., Hider, R. C. (1999) Synthesis, physicochemical characterisation and biological evaluation of 2-(1′-hydroxyalkyl)-3-hydroxypyridin-4-ones: novel iron chelators with enhanced pFe^{3+} values. *J. Med. Chem.* **42**: 4814–4823

Pierre, G. S., Richardson, D. R., Baker, E., Webb, J. (1992) A low-spin iron complex in human melanoma and rat hepatoma cells and a high-spin iron(II) complex in rat hepatoma cells. *Biochim. Biophys. Acta.* **1135**: 154–158

Radisky, D. C., Kaplan, J. (1998) Iron in cytosolic ferritin can be recycled through lysosomal degradation in human fibroblasts. *Biochem. J.* **336**: 201–205

Rae, T. D., Schmidt, P. J., Pufahl, R. A., Culotta, V. C., Ohalloran, T. V. (1999) Undetectable intracellular free copper: the requirement of a copper chaperone for superoxide dismutase. *Science* **284**: 805–808

Rai, B. L., Dekhordi, L. S., Khodr, H., Jin, Y., Liu, Z., Hider, R. C. (1998) Synthesis, physicochemical properties and evaluation of N-substituted-2-alkyl-3-hydroxy-4(1H)-pyridinones. *J. Med. Chem.* **41**: 3347–3359

Sakaida, M. E., Kyle, J. L., Farber, J. L. (1990) Autophagic degradation of protein generates a pool of ferric iron required for the killing of cultured hepatocytes by an oxidative stress. *Mol. Pharmacol.* **37**: 435–442

Taylor, P. D., Morrison, I. E. G., Hider, R. C. (1988) Microcomputer application of nonlinear regression analysis to metal-ligand equilibria. *Talanta* **35**: 507–512

Thomas, F., Serratrice, G., Beguin, C., SaintAman, E., Pierre, J. L., Fontecave, M., Laulhere, J. P. (1999) Calcein as a fluorescent probe for ferric iron. *J. Biol. Chem.* **274**: 13375–13383

Williams, A. T. R., Winfield, S. A., Miller, J. N. (1983) Relative fluorescence quantum yields using a computer controlled luminescence spectrometer. *Analyst* **108**: 1067–1071

Zanninelli, G., Loreal, O., Brissot, P., Konijn, A. M., Slotki, I. N., Hider, R. C., Cabantchik, Z. I. (2002) The labile iron pool of hepatocytes in chronic and acute iron overload and chelator-induced iron deprivation. *J. Hepatol.* **36**: 39–46